

## Practical and Theoretical Analysis of Zero Current Switching (ZCS) - Series Resonant (SR) Inverter Fed High Voltage $D_C$ - $D_C$ Converter

<sup>1</sup>Aamir Amir, <sup>2</sup>Asim Amir, <sup>3</sup>Imran Ahmed

<sup>1</sup>Department of Electronics Engineering, Mehran University of Engineering & Technology, Jamshoro, Pakistan

<sup>2</sup>Department of Electronics Engineering, Institute of Information and Communication Technology, University of Sind, Pakistan

<sup>3</sup>Department of Electronics Engineering, Mehran University of Engineering & Technology, Jamshoro, Pakistan

E-mail: <sup>1</sup>[aamir.a.solangi@gmail.com](mailto:aamir.a.solangi@gmail.com)

### ABSTRACT

This paper presents zero current switching (ZCS) - series resonant (SR) inverter fed, high voltage DC-DC converter with theoretical and practical analysis. The ZCS condition for switching attains almost zero switching losses. Moreover, parasitic oscillations are reduced within the circuit by the resonant tank. Capacitive output filter provides advantages to the circuit, as it is preferred with higher voltage applications. However, at first the peak currents and voltages are a bit problematic, as slight variations in the output voltage and operation at light loads provide limitations to the converter, second the parasitic components within the tank, as the parasitic capacitance and inductance, result into parasitic losses. The system has been analyzed using PSpice software simulations with practical presentation and implementation of the design. The obtained results show that the system has several advantages such as wide range of output voltage control, low output voltage ripple over the entire range and low current stress at light loads; on the contrary the design confronts limitations at peak instants and small loads.

**Keywords:** (ZCS) Zero Current Switching (SR) series resonant, (PWM) Plus width modulation,  $D_C$ - $D_C$  converter

## 1. INTRODUCTION

Power electronics provides an entirely novel platform at power supply designing, as Dc-Dc converter topologies with power components, are widely used as power supplies; these extend applications from commercial to industrial scales including appliances at cottage levels. Full bridge boost converters provide a good approach for higher power applications. Whereas, In case of applications where high output voltages are required in response to low input voltages, current-fed converters are used [1]. The ZCS Dc-Dc converter design provides a novel view to power supplies as reducing switching losses, providing output efficiency and increasing the power density; yet offers a problematic angle. As the non-idealities provided by large turn's ratio of the transformer, leakage inductance and the winding capacitance result to ensure non-idealities in the behavior of the converter. These disorders conclude into undesirable voltage spikes provided by the leakage inductance that may damage circuit components and slow rise times provided by the winding capacitance, which finally results into reduced efficiency and reliability [2, 3, 4, 5]. These non idealities if ignored offer parasitic parameters to the circuit. In consideration to all above parasitic elements many converters have been proposed in past, yet the formal efficiency required is not achieved as the series resonant converter (SRC) not only becomes virtually uncontrollable at light loads but also includes parasitic parameters within the tank circuit providing less efficiency [2, 6, 7]. ZCS-SR converter has been analyzed in response and considering all such parasitic parameters and non-idealities with a tank circuit having two or more resonant components [8, 9].

## 2. PROPOSED DESIGN ANALYSIS

### I. System Architecture and Description

This paper presents a novel view at discontinuous conduction mode (DCM) (LC) series resonant inverter fed high voltage Dc-Dc converter as constructed from three main components, a full-bridge series resonant inverter, a full bridge diode rectifier, both separated by an isolation transformer as shown in Figure.1. The full-bridge inverter section involves four gate controlled semiconductor switches ( $S_1$ ,  $S_2$ ,  $S_3$ , and  $S_4$ ) such as IGBTs, with their connected anti-parallel diodes ( $D_1$ ,  $D_2$ ,  $D_3$ , and  $D_4$ ). As shown in Figure.2. IGBT switches are preferred for discontinuous mode of operation, whereas, MOSFET switches for continuous conduction mode (CCM).

The entire operation of the power supply is objected to achieve a high voltage at the load unit as in Figure.1. Low Dc voltage supplied to the power supply is initially inverted into Ac voltage by the inverter section, the stepping up or down of the voltage as per required is provided by the isolation transformer which besides its preliminary operation also presents an isolation between the supply and the output sections. A full bridge high voltage rectifier connected through the capacitive filter which rectifies the high AC voltage to regulated DC voltage as required by the (load). A capacitive filter is required as the rectified output provided by the full bridge rectifier is discontinuous and contains ripples; so the filter here is chosen to limit the output voltage ripples and spikes, as the output voltage ripple and conversion efficiency are entirely dependent on the operating frequency so the complete circuit gets affected with the spikes at the output of the converter [10].

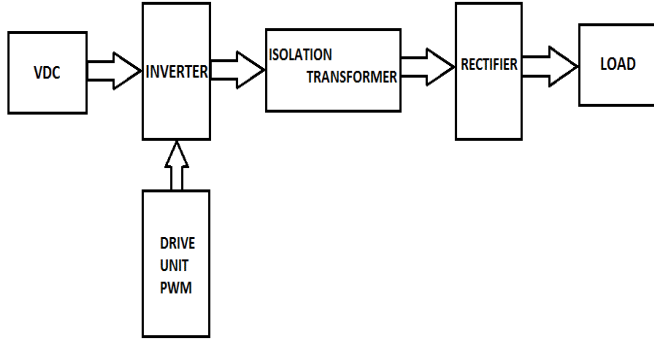


Figure.1. Block diagram

The maximum output voltage (power) is attained with the minimum switching frequency this trade off is achieved by varying the switching frequency, while maintaining a constant break between the pulses simultaneously. At this frequency ZCS (zero current switching) condition is attained for switching of transistors and the optimal operation point for the converter is achieved. We consider the case where:

$$\omega_r = \frac{2\pi}{T_r} = 2\pi f_r \text{ Resonant frequency} \quad (1)$$

$$f_s < 0.5f_r, f_s \text{ Switching frequency} \quad (2)$$

Switches of the ZCS-SR inverter switch ON and OFF due to zero current switching condition as for small time duration the current remains zero through the leakage inductor as the duty ratio is less than 50%. So, the switching frequency is less than half of the resonant frequency; as the entire operation of the ZCS-SR is at fixed frequency and duty ratio.

The parasitic elements as winding capacitance and leakage inductance are disturbing to the behavior of the circuit which are majorly backhanded by the non idealities provided by the transformer due to its heavy insulation requirements and large turn's ratio [11, 12]. These non-idealities result into increased noise and spikes within the current and voltage levels. For utilizing these non-idealities at useful angles, several designs of resonant converters are engaged - as parallel resonant converter (PRC) and series resonant converter (SRC) - presently at work [13, 14]. Each type carries its advantages and disadvantages. Series resonant converters provide a large advantage section as the leakage inductance is absorbed by the resonant circuit and so confronts the probable saturation of the transformer [13, 15]. It sure lessens the disadvantages, yet it is unable to absorb the transformer winding capacitance. In all, the SCR serves its prime principle of providing high output load current at an exceptional efficiency [11, 16, 15, 17].

The series-connected capacitor ( $C_r$ ) and the leakage inductance ( $L_r$ ) of the high-voltage transformers serve as resonant components for ZCS-SR inverter. Assuming ( $C_r$ ) and ( $L_r$ ) as resonant [10], frequency ( $f_r$ ) of the ZCS-SR inverter is given by

Resonant frequency,

$$f_s < 0.5f_r$$

The supply voltage ( $V_S$ ) is

$$V_S = \frac{1}{C_r} \int_{t_0}^t i(t) dt + L_r \frac{di(t)}{dt} + V_p \quad (3)$$

The roots of this RLC circuit are

$$S = \pm \omega_r i \quad (4)$$

Where,

$$\omega_r = \frac{1}{\sqrt{L_r C_r}} \text{ and } i = \sqrt{-1}.$$

$$i = il = ic \quad (5)$$

$$Xl = -Xc \quad (6)$$

$$Z = Xl + Xc \quad (7)$$

Where,

$$Z = j\omega l + \frac{1}{j\omega c} \quad (8)$$

So,

$$\omega_r = \frac{1}{\sqrt{L_r C_r}} \quad (9)$$

$$f_r = \frac{1}{2\pi\sqrt{L_r C_r}} \quad (10)$$

The PWM method is utilized within this design which provides ZCS, consuming the parasitic capacitance and leakage inductance which at switching time intervals provide resonant transitions. This ZCS condition reduces losses majorly at switching levels which term the ZCS-SR converter convenient for high power applications. With phase-shifted PWM method, the gate PWM signals of switches  $S_2$  and  $S_3$  are delayed (phase-shifted) with respect to those of the switches  $S_1$  and  $S_4$ ; as shown in Figure.3.

Operations for a series resonant converter (SRC) constant on-time phase-shifted PWM are defined as: the discontinuous conduction mode (DCM) and continuous conduction mode (CCM). In this paper a view at DCM operation is taken into consideration as the switching frequency is less than half of the resonant frequency. The inductor current remains at zero for a small interval to display discontinuity as shown in Figure.4. [11].

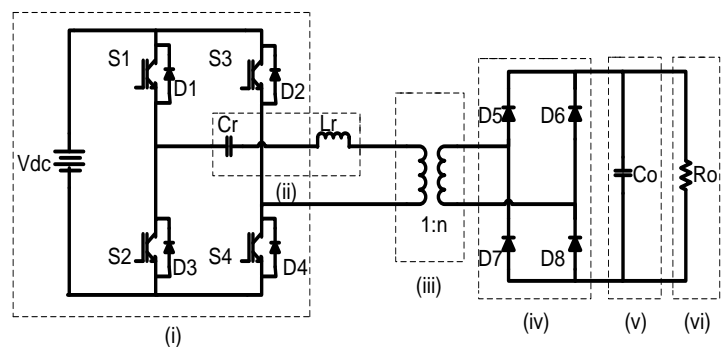


Figure.2. Schematic diagram of the ZCS SR inverter fed high voltage DC-DC converter

(i) Inverter, (ii) Series Resonant circuit, (iii) Isolation Transformer, (iv) Diode Rectifier, (v) Capacitive Filter, (vi) Load Resistance.

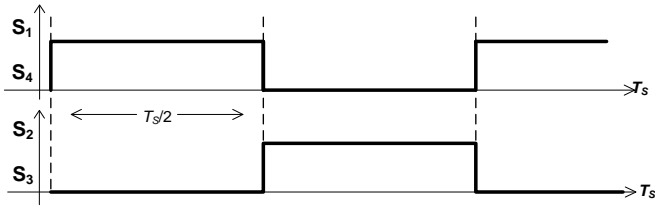


Figure.3. Phase shift PWM control wave form.

## II. Steady-state analysis

PWM method can be opted for the analysis of the ZCS-SR inverter, as the switches (S1, S2, S3, and S4) utilized in the inverter are driven in a diagonal fashion, output voltage can only be provided to the load unit during ON time consideration of the switches; which corresponds to a specific duty cycle when operated at fixed frequency. Ideally the full bridge inverter operates at 50% duty cycles but practically depends on the application required [18].

Figure.2. shows the complete circuit with its six fractions and simulated waveforms of the inductor current and capacitive voltage can be analyzed from Figure.4. As the Period analyzed is  $(t_0-T_s)$  displaying the device voltage and current.

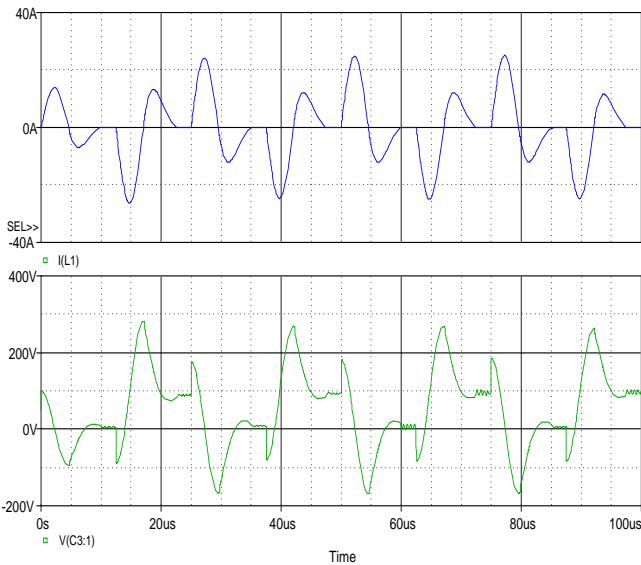


Figure.4. Steady-state waveforms of the system design for resonant inductance and capacitance, current and voltage, respectively.

Considering Figure.4. The cycle from  $25\mu\text{s}$  to  $48\mu\text{s}$  ( $t_0-t_5$ ) and breaking into intervals to form modes of operation as:

### A. Mode I

As shown in Figure.5. Mode I extends from  $(t_0-t_1)$ , during the positive cycle of operation, the switches  $S_1-S_4$  are switched ON, allowing a path to the input voltage to travel at the output through the LC tank circuit. Approximately, half-sinusoidal current flows through the switches  $S_1-S_4$ , these switches instantaneously turn OFF at the time  $(t_1)$ .

### B. Mode II

As shown in Figure.6. Mode II operates from  $(t_1-t_2)$ , energy stored in the tank during Mode I travels back to the  $D_C$  source and power is supplied to the load from time  $(t_1-t_2)$ . Bidirectional energy flow; cannot occur because diodes  $D_1-D_4$  connected in anti-parallel and so can only allow unidirectional energy transfer, switches  $S_1$  and  $S_4$  remain OFF under ZCS condition. In all; the resonant current flows in the reverse direction.

### C. Mode III

As shown in Figure.7. from time  $(t_3-t_4)$  Mode III, as from  $(t_2-t_3)$  discontinuity sustains which is shown in Figure.4 to present DCM operation. In this mode  $D_C$  source supplies power to the load resistance. During the negative half cycle  $S_2$  and  $S_3$  turn ON at ZCS.

### D. Mode IV

As shown in Figure.8. finally from  $(t_4-t_5)$ , works in similar fashion to Mode II for the negative cycle of operation. Energy stored during Mode-III in the resonant circuit now flows in the reverse direction. Diodes  $D_2-D_3$  connected anti-parallel to the switches  $S_2$  and  $S_3$  obstruct the reverse flow of current turning OFF switches  $S_2$  and  $S_3$  under ZCS.

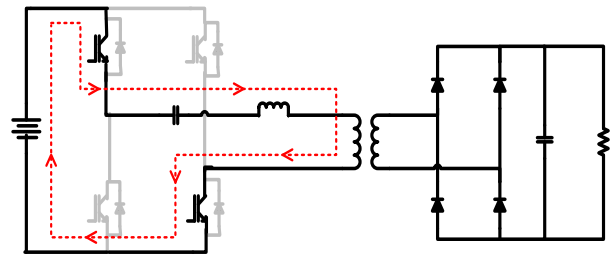


Figure.5. The equivalent circuit of Mode I

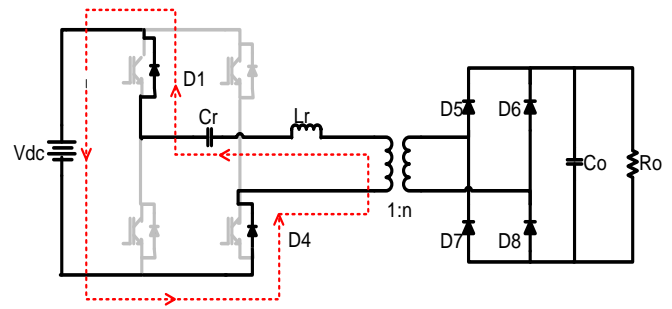


Figure.6. The equivalent circuit of Mode II

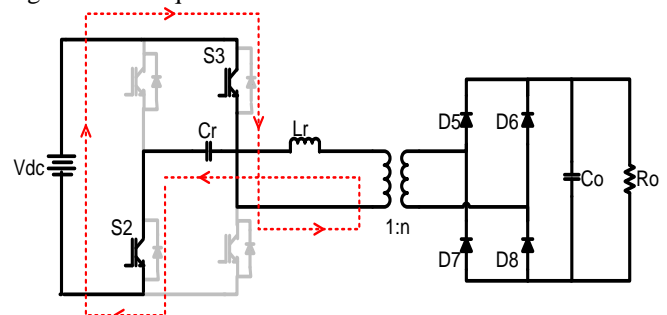


Figure.7. The equivalent circuit of Mode III

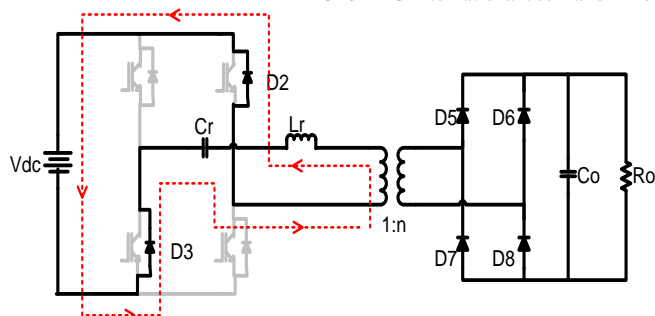


Figure.8. The equivalent circuit of Mode IV

Finally for smooth and ripple free Dc voltage at the output the high frequency Ac voltage which can be estimated from the turn's ratio; is rectified and filtered with a low-pass filter.

### 3. SIMULATION RESULTS AND EVALUATION

In order to confirm that the proposed zero current switching (ZCS) - series resonant (SR) inverter fed high voltage DC-DC converters can be practically implemented, simulation verification was performed to verify the results by using Pspice software. The details of the proposed simulation system are as follow: Input voltage,  $V_{DC} = 100$  V dc, Resonant capacitance,  $C_r = 200$  nF, resonant inductance,  $L_r = 10$  uF, Switching frequency,  $f_s = 40$  kHz, Resonant frequency,  $f_r = 112$  kHz, Load resistance,  $R_o = 100$  k $\Omega$ , 500 k $\Omega$  & 1M $\Omega$ . The turn's ratio of high voltage transformer is 300. The proposed circuit was simulated for wide range of output voltage and load settings. With 200nF capacitance of the resonant tank circuit and corresponding resonant frequency 112 kHz, the converter would operate in discontinuous conduction mode up to switching frequency of 40 kHz. The output load resistance for this case is varied to 100k $\Omega$ , 500k $\Omega$  and 1M $\Omega$ .

Now for load resistance  $R_o = 100$  k $\Omega$  It can be seen from the Figure.9, that the output voltage of the converter is approximately 15 kV and peak resonant current is 125 A. The output power of high voltage dc-dc converter is approximately 2.1 kW. Furthermore, the current through inverter remains zero for a small duration after every resonant period, thus resonant inverter is operating in discontinuous conduction mode, so the switching loss is minimized.

The simulated waveforms in Figure.10, show the output voltage of converter approximately 65 kV and peak inverter current 125A and current though the inverter is discontinuous. The output power of converter in this case is 9 kW where the load resistance value was varied to 500k $\Omega$ .

If the load resistance is again varied to 1M $\Omega$  the obtained waveforms of output voltage and inverter current, show in Figure.11, that output voltage of converter for this case is approximately 110 kV, peak inductor current is 125 A and output power is 12.70W. This proves that the converter is able to control its output voltage over wide range.

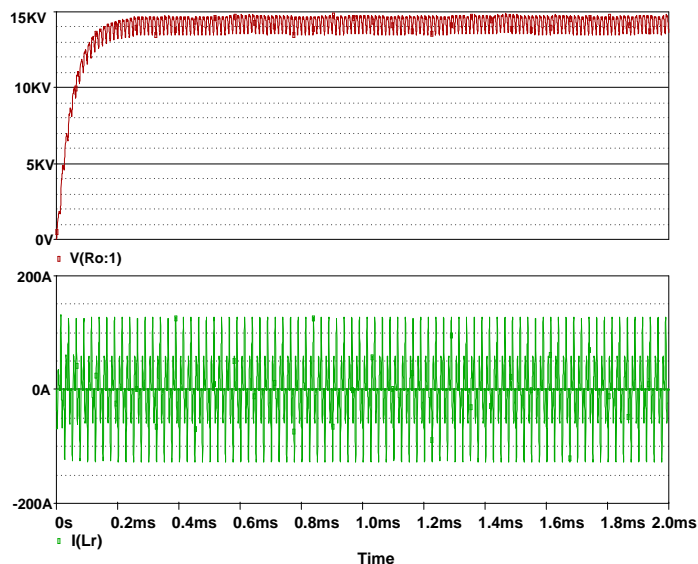


Figure.9. Simulation result of the output voltages and output currents of the proposed converter for  $R_o = 100$  k $\Omega$ .

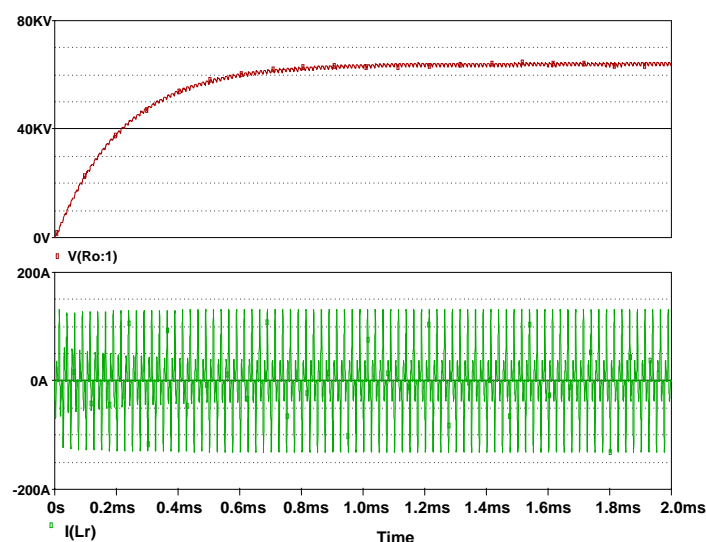


Figure.10. Simulation result of the output voltages and output currents of the proposed converter at  $R_o = 500$  k $\Omega$ .

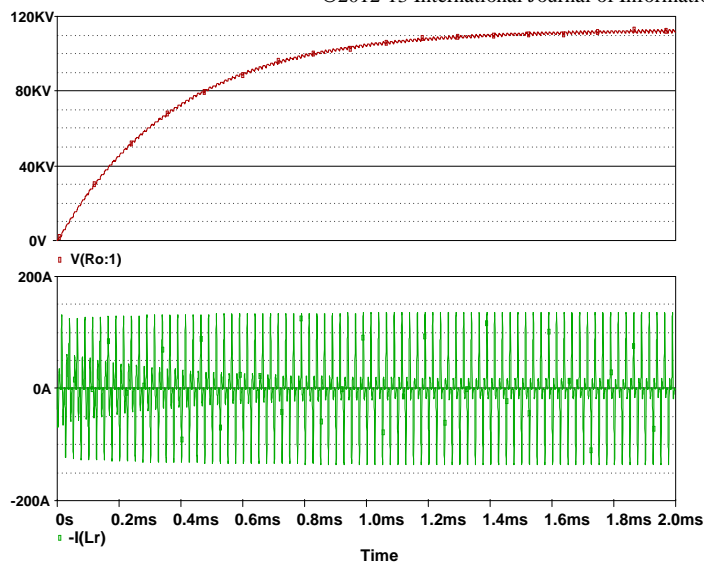


Figure.11. Simulation result of the output voltages and output currents of the proposed converter for  $R_o = 1M\Omega$ .

#### 4. PRACTICAL IMPLEMENTATION

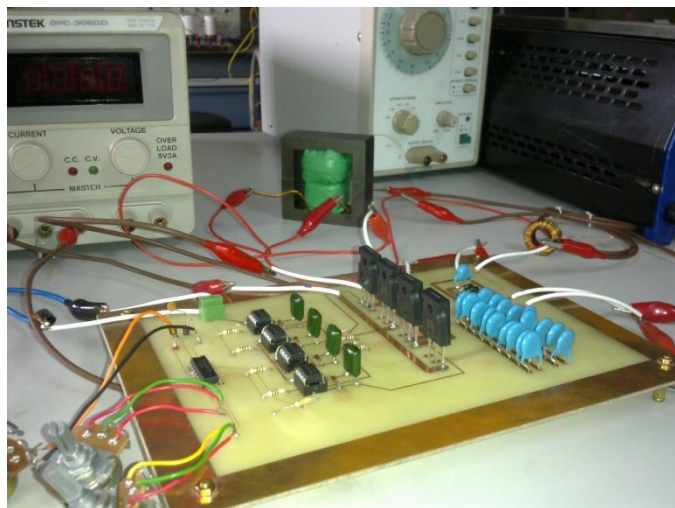


Figure.12. Practical model of the ZCS-SR Dc-Dc converter.

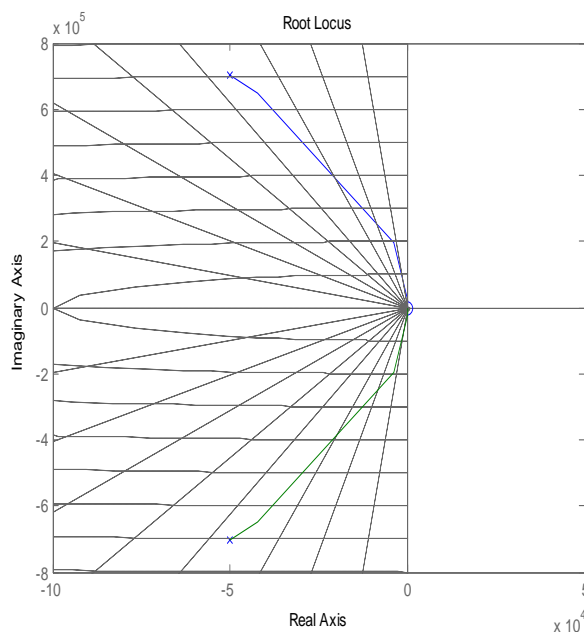


Figure.13. Root Locus of the proposed model.

#### 5. CONCLUSION

The analysis of the Zero Current Switch (ZCS) - series resonant (SR) inverter fed, high voltage DC-DC converter through theoretical and practical measures has been presented, and results have been presented to evaluate the performance of the converter with practical implementation of the design. The analysis affirms a design with increased efficiency, better power density and switching effectiveness, as shown using Pspice simulation software. These results show that the proposed converter can be used for high power applications which give constant dc output voltage with fewer losses, but confronts limitations as the formal efficiency required is not yet achieved, as it becomes almost virtually uncontrollable at light loads, the voltage and current spikes produced and most of all the slow rise time which sum up to provide resistivity against an efficient performance. The design can be improved by adding a parallel tank circuit in series with the design presented in this paper, which would ensure eradication of the voltage spikes and the slow rise time. Thus, resulting into a further efficient system; implementable for light loads.

#### ACKNOWLEDGEMENTS

The authors acknowledge the Mehran university of Engineering & Technology, Jamshoro, Pakistan, for providing laboratory and research facilities.

#### REFERENCES

- [1] S.Ajitha and N.Kalaiarasi. Article: Implementation of Full-Bridge Current-Fed Resonant Boost Converter using PIC microcontroller. International Journal of Computer Applications 1(7):76-81, February 2010. Published By Foundation of Computer Science.

- [2] Iannello, C.; Luo, S.; Batarseh, I.; , "Full bridge ZCS PWM converter for high-voltage high-power applications," *Aerospace and Electronic Systems, IEEE Transactions on* , vol.38, no.2, pp.515-526, Apr 2002
- [3] Weinberg, A. H., and Schreuders, J. (1986) A high-power high-voltage dc-dc converter for space applications. *IEEE Transactions on Power Electronics*, **E-I**, 3 (July 1986), 148—160.
- [4] Johnson, S. D., et al. (1988) Comparison of resonant topologies in high-voltage dc application. *IEEE Transactions on Aerospace and Electronic Systems*, **24**, 3 (May 1988), 263—274.
- [5] Krichtafovitch, I. A., and Sinitsyna, I. Z. (1994) Theory and design of high-voltage power supplies. *HFPC'95*, 147—157.
- [6] Kim, Y. J., et al. (1995) Comparative performance evaluations of high-voltage transformer parasitic parameter resonant inverter-linked high-power dc-dc converter with phase-shifted PWM scheme. *PESC'95*, 120—127.
- [7] Jacobson, B. S., and Dipema, R. A. (1993) Fixed frequency resonant converter for high voltage high density applications. *PESC'93*, 357—363.
- [8] Garcia, V., et al. (1994) An optimized dc-to-dc converter topology for high-voltage pulse-load applications. *PESC'94*, 1413—1421.
- [9] Vlatkovic, V., et al. (1996) Auxiliary series resonant converter: A new converter for high-voltage, high-power applications. *IEEE APEC'96*, 493—499.
- [10] Iqbal, S.; Singh, G.K.; Besar, R.; , "A Dual-Mode Input Voltage Modulation Control Scheme for Voltage Multiplier Based X-Ray Power Supply," *Power Electronics, IEEE Transactions on* , vol.23, no.2, pp.1003-1008, March 2008 doi: 10.1109/TPEL.2008.917820
- [11] J. Sun, X. Ding, M. Nakaoka, and H. Takano, "Series resonant ZCSPFM DC-DC converter with multistage rectified voltage multiplier and dual-mode PFM control scheme for medical-use high-voltage X-ray power generator," *Proc. Inst. Elect. Eng., Elect. Power Applicat.*, vol. 147, no. 6, pp. 527-534, Nov. 2000.
- [12] S. Iqbal, R. Besar, and C. Venkateshaiah, "A Dual-Mode Phase-Shift Modulation Control Scheme for Voltage Multiplier Based X-Ray Power Supply," *Journal of Instrumentation* , vol.5, no.5, pp.TO5001, May 2010.
- [13] R. L. Steigerwald, "High-Frequency Resonant Transistor DC-DC Converters," *IEEE Trans. Ind. Electron.*, vol.IE-31, no.2, pp.181-191, May 1984
- [14] H. Takano, and T. Hatakevama, "Feasible characteristics evaluation of resonant PWM inverter-linked dc-dc power converter using high-voltage transformer parasitic circuit components," in *6th Int. Conf. on Power Electron. And Variable Speed Drives*, 1996, pp. 525-533.
- [15] T. F. Wu, and J. C. Hung, "A PDM controlled series resonant multilevel converter applied for X-ray generator," in *IEEE Power Electron. Specialists Conf.*, vol. 2, 1999, pp. 1177-1182.
- [16] S. Iqbal, G. K. Singh and R. Besar, "A Dual-Mode Input Voltage Modulation control scheme for Voltage Multiplier Based X-ray Power Supply," *IEEE Trans. Power Electron.*, vol. 23, no. 2, pp. 1003-1008, March 2008.
- [17] K. Ogura, E. Chu, M. Ishitobi, M. Nakamura, and M. Nakaoka, "Inductor snubber-assisted series resonant ZCS-PFM high frequency inverter link DC-DC converter with voltage multiplier" in *IEEE Power Convers. Conf.*, 2002, pp. 110-114.
- [18] Sze Sing Lee; Iqbal, S.; Kamarol, M.; , "Control of ZCS-SR Inverter-Fed Voltage Multiplier-Based High-Voltage DC-DC Converter by Digitally Tuning Tank Capacitance and Slightly Varying Pulse Frequency," *Power Electronics, IEEE Transactions on* , vol.27, no.3, pp.1076-1083, March 2012